

Trends in NMR Logging

During the past decade, the remarkable technology of nuclear magnetic resonance (NMR) logging has improved continually. Oil companies are using NMR measurements for an ever-growing number and range of applications, such as characterizing formation fluids during reservoir evaluation and assessing formation producibility. Now the measurements provided by these tools are dramatically changing well-completion designs and reservoir development.

David Allen
Charles Flaum
T. S. Ramakrishnan
Ridgefield, Connecticut, USA

Jonathan Bedford
London, England

Kees Castelijns
New Orleans, Louisiana, USA

David Fairhurst
San Antonio, Texas, USA

Greg Gubelin
Nick Heaton
Chanh Cao Minh
Sugar Land, Texas

Mark A. Norville
Milton R. Seim
Kerns Oil and Gas, Inc.
San Antonio, Texas

Tim Pritchard
BG Group plc
Reading, England

Raghu Ramamoorthy
Kuala Lumpur, Malaysia

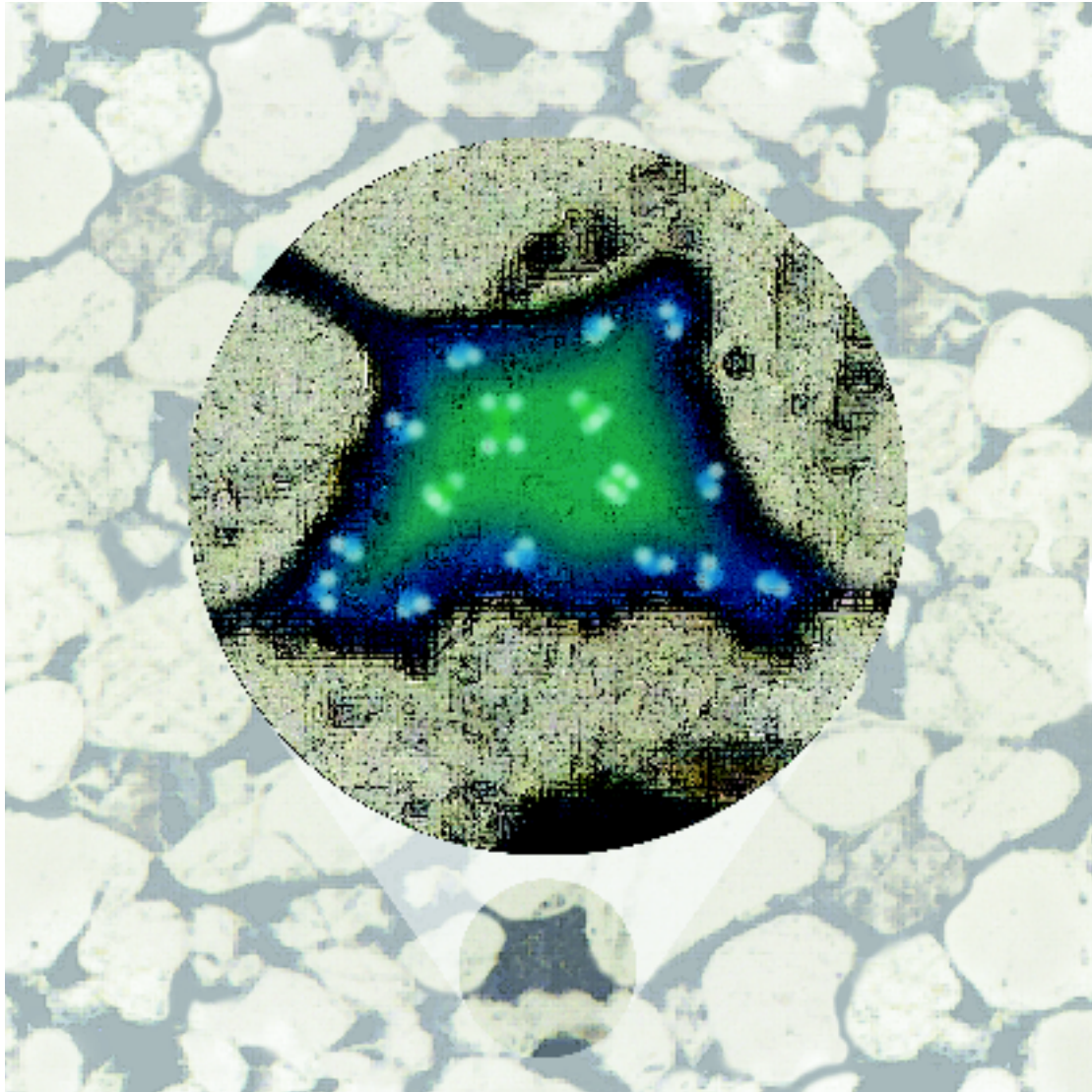
For help in preparation of this article, thanks to Rob Badry, Calgary, Alberta, Canada; Kamel Bennaceur, Dylan Davies, Robert Freedman and Bruce Kaiser, Sugar Land, Texas, USA; Dale Logan, Midland, Texas; Robert Kleinberg, Ridgefield, Connecticut, USA; Don McKeon, Montrouge, France; LSD Onuigbo, Lagos, Nigeria; and Lee Ramsey and Frank Shray, Houston, Texas.

CMR, CMR-200, CMR-Plus (Combinable Magnetic Resonance), DMR (Density-Magnetic Resonance Interpretation Method), FracCADE, FMI (Fullbore Formation MicroImager), MDT (Modular Formation Dynamics Tester), OFA (Optical Fluid Analyzer), PowerSTIM and TLC (Tough Logging Conditions) are marks of Schlumberger. MRIL and MRIL-Prime are marks of NUMAR Corporation.

In the last decade, petrophysicists applauded the newly arrived pulsed nuclear magnetic resonance (NMR) logging tools for their ability to solve difficult formation-evaluation problems. Service companies continue to invest significant research effort into refining NMR measurements. The result has been a steady stream of tool advancements and new applications. In the mid-1990s, the introduction of higher rate pulsing

techniques extended the fluid-mobility characterization capabilities of these tools. Recently, there have been impressive improvements in data-acquisition capabilities, which have led to significant increases in logging speeds.

A fundamental advantage of the latest generation of NMR tools is the ability to provide a wider scope of information about reservoirs than ever before. NMR data can answer many key questions for nearly everyone involved in

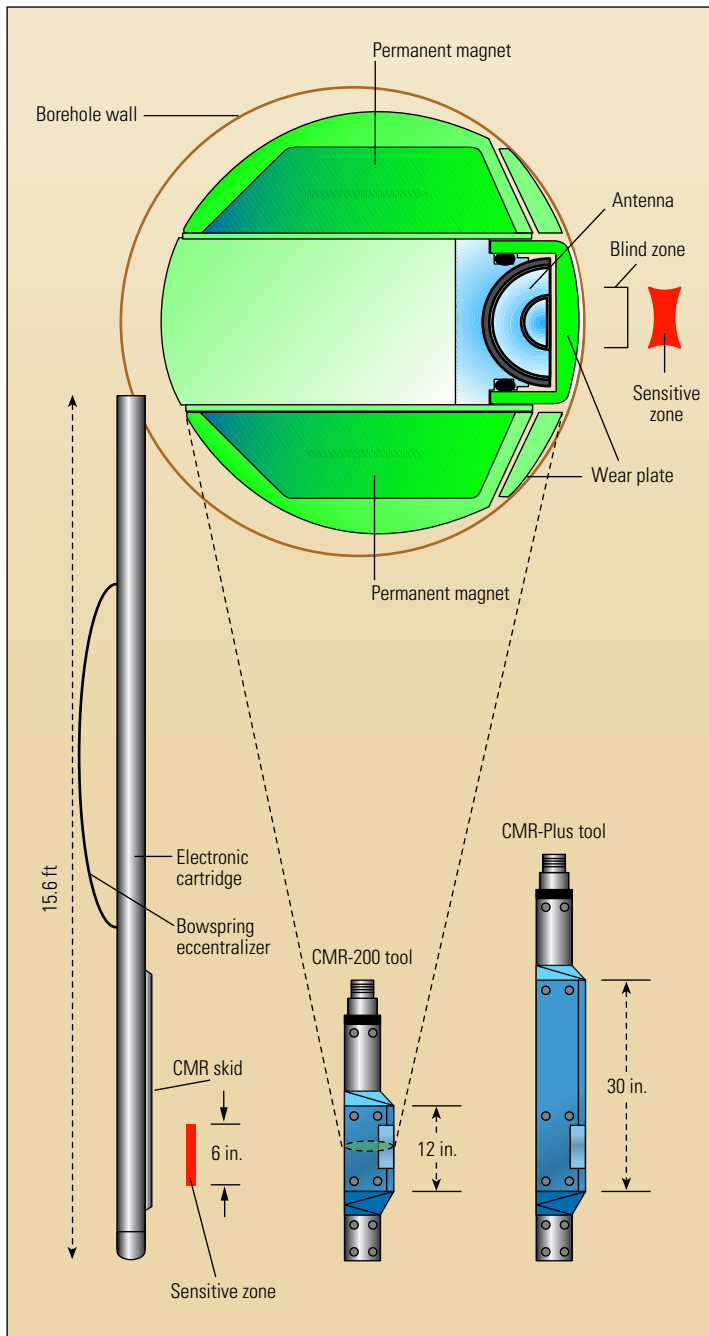


exploration and production, including reservoir engineers, completion engineers, geologists and petrophysicists. For example, completion engineers now use NMR measurements to design hydraulic-fracture treatments for reservoir stimulation. Reservoir engineers assess rock quality with high-resolution NMR data to locate vertical permeability barriers and improve production management. Geologists and petrophysicists

have an improved understanding of pore geometry for depositional analysis from decay-time distributions. Hydrocarbon characterization is also improved by interpreting NMR logs in combination with other logging measurements. The result is a more accurate evaluation of well producibility.

This article first reviews recent advances in NMR tool technology and discusses how some of these developments, such as enhanced precision,

increased logging speed and high-resolution measurements, are leading to new NMR applications. Field examples show how this information is used to design well completions, and how NMR and data from wireline formation testers are providing highly efficient, low-risk ways to evaluate well producibility. Finally, we discuss the latest developments in evaluating carbonate formations with NMR.



▲ CMR tool design. The CMR-Plus tool uses a similar antenna, magnet configuration and electronics as the CMR-200 tool. The pair of permanent magnets creates a resonant-field sensitive zone in the formation (*top right and lower left*). However, the CMR-Plus magnets (*lower right*) are 30 in. [76 cm] long to provide prepolarization of the hydrogen spins while logging continuously. This new design feature allows the CMR-Plus tool to log faster.

New Tool Advances

The CMR Combinable Magnetic Resonance tool, introduced by Schlumberger in 1995, is run pressed against the borehole by a bowspring. A short directional antenna sandwiched between a pair of optimized magnets focuses the CMR measurement on a 6-in. [15-cm] vertical zone located 1.1 in. [2.8 cm] inside the formation. These features and the tool's enhanced signal-to-noise data-acquisition electronics provide accurate, high-precision measurements in the formation with high vertical resolution.¹

With the increased price of crude oil and substantial rig rates offshore, it's more important than ever to be able to make decisions rapidly. The latest addition to the CMR family of tools, the CMR-Plus tool, addresses this need (*left*). The new tool includes several improvements over its predecessor, the CMR-200 tool, including a new magnet design with a longer prepolarizing field that increases logging speeds to 3600 ft/hr [1097 m/hr] in fast-relaxation environments. This compact, lightweight, rugged tool is 15.6 ft [4.8 m] long and weighs 450 lbm [204 kg]. A low-profile skid design allows logging in holes as small as 5½ in. [15 cm]. A new pulse-acquisition sequence, called the enhanced-precision mode (EPM), is coupled with an upgraded electronics package to increase the signal-to-noise ratio and improve high-precision measurements for evaluating reservoirs (*next page, top*).²

The ability to make fast, high-precision NMR measurements is changing the way that engineers perceive the producibility of their wells. For example, zones that might have been considered unproductive because of high water saturation and the potential for producing excessive water might, in fact, be worth examining to determine if the water is immovable. For example, in a development well in South America, a CMR-Plus log revealed that a zone of apparent high water saturation was irreducible—the formation would produce water-free hydrocarbons. Previously, the operator had bypassed this zone during field development. Based on the new information, the operator perforated the zone and produced dry gas, adding 20 Bcf [566 million m³] of gas reserves.

The higher logging speeds made possible by the CMR-Plus tool enables operators to economically acquire data over longer intervals that include zones that initially were of little interest.

NUMAR Corporation, a subsidiary of Halliburton, developed the MRIL Magnetic Resonance Imaging tool, which incorporates a long permanent magnet to create a static lateral field in the formation. This tool is run centralized in the borehole, and the measurement volume consists of a concentric cylindrical resonant shell with a length

1. Allen D, Crary S, Freedman B, Andreani M, Klopff W, Badry R, Flaum C, Kenyon B, Kleinberg R, Gossenberger P, Horkowitz J, Logan D, Singer J and White J: "How to Use Borehole Nuclear Magnetic Resonance," *Oilfield Review* 9, no. 2 (Summer 1997): 34-57.

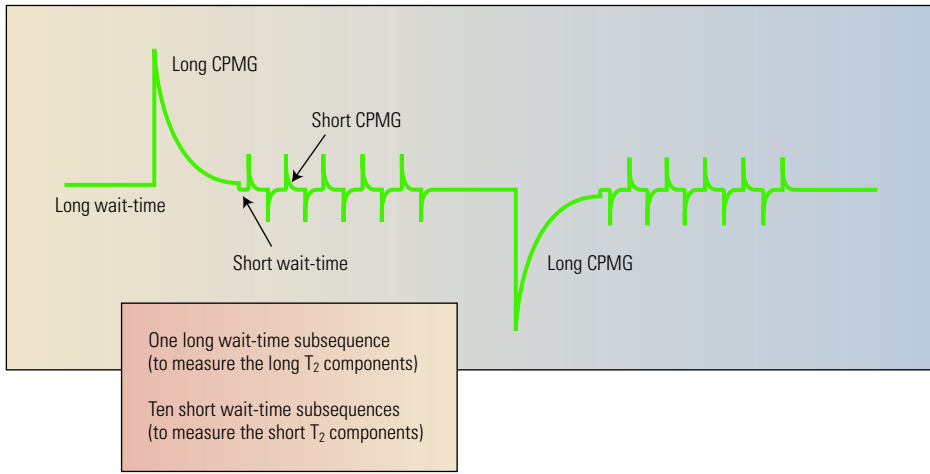
2. Freedman, R: "Dual-Wait Time Processing for More Accurate Total and Bound Fluid Porosity," U.S. Patent Application 156,417, 1998.

McKeon D, Cao Minh C, Freedman R, Harris R, Willis D, Davies D, Gubelin G, Oldigs R and Hurlimann M: "An Improved NMR Tool for Faster Logging," *Transactions of the SPWLA 40th Annual Logging Symposium*, Oslo, Norway, May 30-June 3, 1999, paper CC.

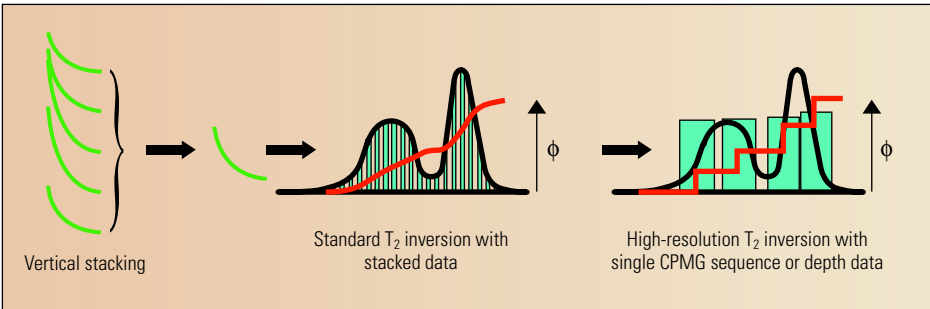
3. Prammer MG, Bouton J, Chandler RN and Drack ED: "Theory and Operation of a New Multi-Volume NMR Logging System," *Transactions of the SPWLA 40th Annual Logging Symposium*, Oslo, Norway, May 30-June 3, 1999, paper DD.

4. Coates G and Denoo S: "The Producibility Answer Product," *The Technical Review* 29, no. 2 (1981): 54-63.

5. Heaton N, Cao Minh C, Freedman R and Flaum C: "High Resolution Bound-Fluid, Free-Fluid and Total Porosity with Fast NMR Logging," *Transactions of the SPWLA 41st Annual Logging Symposium*, Dallas, Texas, USA, June 4-7, 2000, paper V.



^ Enhanced-precision mode (EPM). The EPM measurement is a new multiwait Carr-Purcell-Meiboom-Gill (CPMG) pulse-echo acquisition sequence designed to improve the short T_2 , or bound-fluid, measurement precision. The EPM measurement consists of one long wait-time pulse sequence that measures all the T_2 components, followed by a series of short wait-time sequences optimized for the early T_2 components from small pores. The short wait-time sequences are stacked to decrease the noise of the measurement, resulting in greater precision in the early echo data. This improves the precision in the bound-fluid volume and total CMR porosity measurements.



^ High-resolution, multilevel data-windows processing. Vertical stacking (*left*) of echo trains and inversion are used to obtain a T_2 distribution (*middle*) for the averaged data. An equivalent T_2 distribution is formed with a reduced number of T_2 bins of approximately equal amplitude (*right*). The total porosity, ϕ , and logarithmic mean T_2 value of the reduced distribution are identical to those of the original distribution.

of 24 in. [61 cm], and a thickness of approximately 0.04 in. [1 mm]. The average diameter of the resonant shell is about 15 in. [40 cm] and is set by the operating frequency of the tool. In a 10-in. [25.4-cm] borehole, this leads to a depth of investigation (DOI) of 2.5 in. [7.6 cm]. A large DOI helps reduce the sensitivity to rugosity in many boreholes.

The latest version of the NUMAR tool, the MRIL-Prime, incorporates improvements to increase logging speed and efficiency.³ It has 3-ft [1-m] prepolarizing magnets both above and below the antenna for logging upward and downward, and a nine-frequency multishell measurement capability. Each measurement shell can be programmed with a different pulse sequence, and the

measurement can be switched between different shells by changing the frequency. The total variation in the depth of investigation of the nine shells is about 1 in. [2.5 cm]. The multifrequency operation provides a total porosity measurement, and multiparameter data acquisition with different pulsing sequences in each shell.

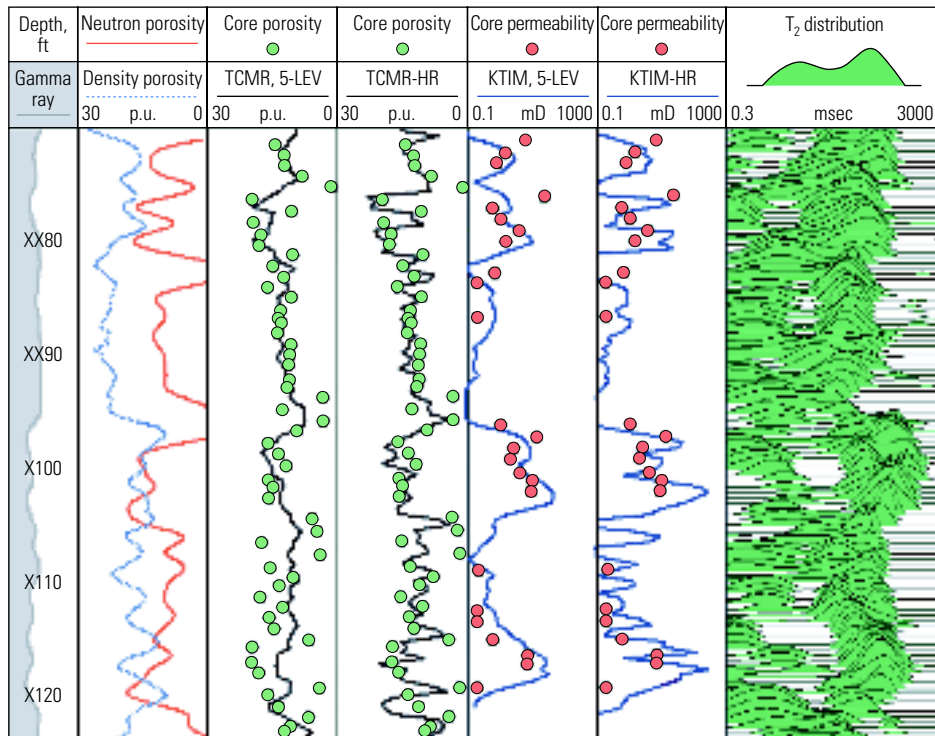
The tool is available in two sizes. The standard tool diameter is 6 in.; the length is 53 ft [16 m]; and the weight is 1500 lbm [680 kg]. A slim tool has a 4 $\frac{7}{8}$ -in. [12-cm] diameter, is 50 ft [15 m] long, and weighs 1300 lbm [590 kg]. These tools enable logging in hole sizes from 5 $\frac{7}{8}$ in. to 12 $\frac{1}{4}$ in. [31 cm]. Logging speed in short-polarization-time environments is 1440 ft/hr [440 m/hr], and 700 ft/hr [213 m/hr] for the slim version of the tool.

High-Resolution NMR

The identification and quantification of rock geometry and fluid mobility on the basis of the fluid's nuclear spin relaxation characteristics are among the most important contributions of NMR logging. The separation of porosity into bound-fluid and free-fluid components is essential for evaluating reservoir producibility.⁴ In thin, laminated formations, producibility depends not only on the net ratio of bound-fluid to free-fluid volumes, but also on the relative location of the two fluid volumes within the different laminated beds. Measurements are useful in this capacity only if they are sensitive to spatial variations on a length scale comparable to the lamination thickness. The production engineer can use high-resolution NMR data to evaluate producibility of thinly laminated sections, obtain accurate hydrocarbon pore volume and identify vertical permeability barriers that can help avoid producing undesired water from nearby aquifers. The completions engineer can use high-resolution data to accurately position perforating, fracturing and formation stimulation designs.

High-resolution producibility—The vertical resolution of an NMR measurement is determined by the antenna length, the acquisition sequence signal-to-noise ratio and the logging speed. For example, CMR-200 tool measurements combine overlapping phase-alternated pairs (PAP) of Carr-Purcell-Meiboom-Gill (CPMG) pulse-echo sequences and a short antenna to resolve beds as thin as 6 in. (see "Basics of NMR Logging," page 12). The long prepolarization magnet in the CMR-Plus tool allows nonoverlapping PAP measurement acquisition at logging speeds up to 3600 ft/hr with only a minor reduction in vertical resolution. In practice, the vertical resolution for most NMR measurements is degraded by the depth-stacking technique used to improve the signal-to-noise ratio necessary for T_2 -inversion processing.

Recent developments in high spatial-resolution CMR logging stem from a new processing method optimized for high-resolution answers and an EPM data-acquisition scheme.⁵ In high-resolution processing, T_2 inversion is performed without applying any vertical averaging of the echo data. The high-resolution inversion procedure differs from standard inversion in several aspects. Standard inversion typically uses between 30 and 50 T_2 components, which encompass the entire range of possible relaxation times exhibited by formation and drilling fluids. High-resolution processing uses only two to five T_2 components (*above left*). Furthermore, these



^ Australian well with thinly bedded sand-shale sequence. Traditional density (blue) and neutron (red) logs are shown in Track 1. A five-level averaged CMR total porosity (black) is compared with core porosity in Track 2. The high-resolution CMR total porosity (black) is compared with core porosity in Track 3. Note how well the high-resolution total porosity captures the sharp porosity variations seen throughout the core data. The five-level averaged CMR permeability (blue) is compared with core data in Track 4, and the high-resolution permeability (blue) in Track 5. Again, the high-resolution CMR log agrees well with the permeability variations seen in the core data. A gamma ray log is shown in the depth track, and the CMR T₂ distributions are shown in Track 6.

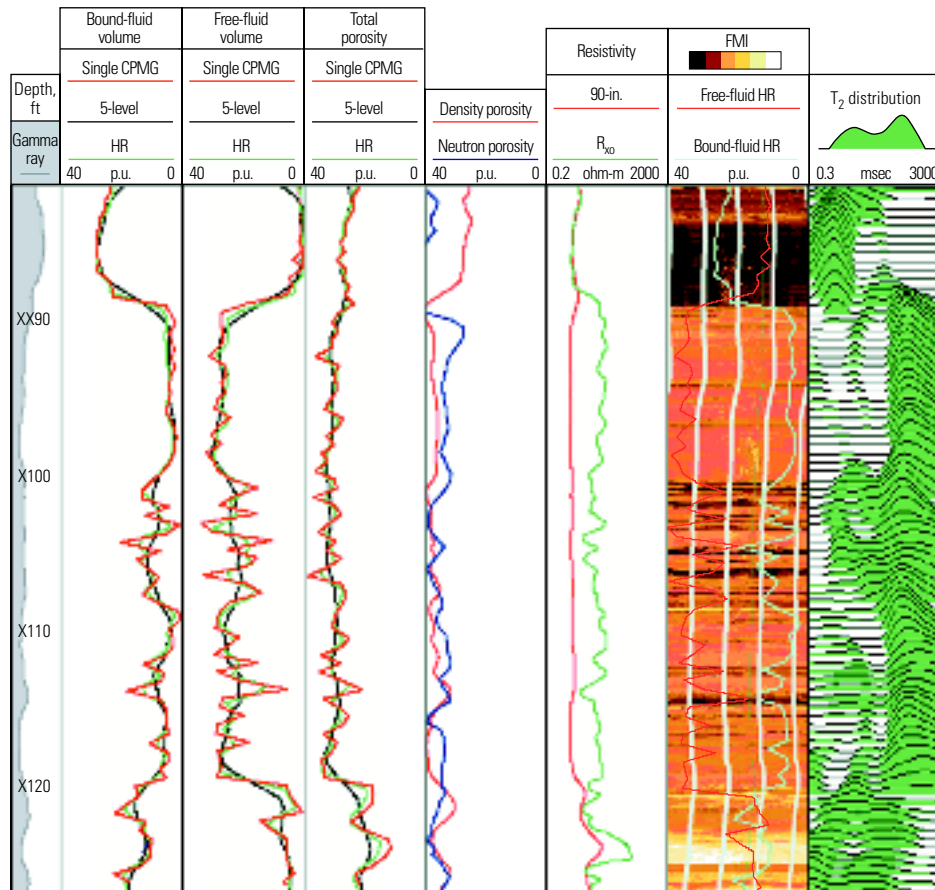
components are selected by analysis of the standard T₂ distribution obtained from the stacked data at each depth.

For example, if the stacking interval at a particular depth consists of a clean sand giving a single peak in the T₂ distribution centered between 50 and 300 msec, then the T₂ components used in the high-resolution inversion will be derived entirely from this range. By using a small number of “optimal” T₂ values, the high-resolution inversion provides total porosity with high precision. To ensure accuracy and consistency with standard processing, the high-resolution porosity is scaled such that the mean value matches that of the

standard porosity. This strategy is similar to the alpha-processing method used to derive high-resolution density measurements.⁶

Separation of the high-resolution porosity into bound- and free-fluid volumes is straightforward. Because the free-fluid signal decays slowly, it contributes to a large number of echoes. Consequently, the free-fluid volume can be computed with high precision using standard inversion without stacking the data. This provides a high-resolution free-fluid volume estimate. A high-resolution bound-fluid volume is obtained as the difference between the high-resolution total porosity and the high-resolution free-fluid volume.

High-resolution NMR porosity and permeability data are essential for evaluating thinly laminated reservoirs. For example, data in an Australian well drilled in a thinly bedded sand-shale sequence show little correlation between core porosity and the openhole neutron and density porosity logs (above). The core porosity displays large fluctuations in the lower zone—as much as 20 p.u. over a 1-ft [0.3-m] interval, as might be expected in a laminated formation. In such zones, traditional openhole logs and traditional NMR logging with three- or five-level averaging often provide inadequate vertical resolution and limited ability to pick zones for perforating.



▲ High-resolution NMR log correlation with FMI images. In Tracks 1 to 3, the traditional bound-fluid, free-fluid and total porosity logs processed with five-level depth averaging (black) are compared with high-resolution curves (green), and corresponding single CPMG-derived estimates (red). Neutron (blue) and density (red) porosity logs are shown in Track 4 and the deep (red) and shallow (green) resistivity logs are shown in Track 5. Over the top zone, from XX90 to X100 ft, the high-resolution logs are relatively featureless and overlie the averaged logs. However, in the lower zone from X100 to X120 ft, the high-resolution logs show increased activity due to the fine laminations that are apparent in the FMI image shown in Track 6. Note that the bound-fluid and free-fluid logs anticorrelate, and compensate for one another, leading to a total porosity log that provides little indication of the laminations. The substantial fluctuations in free fluid and bound fluid in the lower section correlate well with the laminations apparent in the FMI image.

The high-resolution total CMR porosity, plotted in Track 3, captures the sharp porosity fluctuations and agrees well with the core data. The high-resolution Timur-Coates permeability estimates derived from the CMR measurements also compare favorably with the core permeabilities shown in Track 5. Timur-Coates permeability estimates are discussed in detail below.

In Canada, the CMR-Plus tool was run at 1200 ft/hr [366 m/hr] in a shaly-sand formation with fine laminations (above). The high-resolution free-fluid and bound-fluid volume logs correlate well with the fine laminations shown by the FMI Fullbore Formation Microlmager display in the lower zone. In this well, the high-resolution free-

and bound-fluid logs anticorrelate and compensate each other so much that the high-resolution total porosity log provides little indication of the laminations. Single CPMG estimates further enhance resolution, most notably over the section from X100 ft to X120 ft. The high-resolution CMR logs in the upper zone from XX90 ft to X100 ft overlie the traditionally processed logs and show little evidence of laminated beds.

This example demonstrates that robust high-resolution NMR logs can be obtained with the CMR-Plus tool at fast logging speeds using this innovative processing technique. Laminations of 4 to 6 in. [10 to 15 cm] are resolvable, and precisely locate the thin, high-porosity pay zones between the shale beds.

High-precision permeability indicator— Another important contribution of NMR logging is its capability to provide a continuous permeability measurement. In thinly laminated formations, permeability can vary by orders of magnitude within a few inches. Under these conditions, it is important to obtain a continuous permeability estimate with the highest possible depth resolution. The two widely applied permeability transforms used today, based on NMR

6. Galford JE, Flaum C, Gilchrist WA and Duckett S: "Enhanced Resolution Processing of Compensated Neutron Logs," paper SPE 15541, presented at the SPE Annual Technical Conference and Exhibition, New Orleans, Louisiana, USA, October 5-8, 1986.

| Timur-Coates equation | SDR equation |
|---------------------------------|---------------------------------|
| $k_{TIM} = a\phi^m (FFV/BFV)^n$ | $k_{SDR} = b\phi^m (T_{2LM})^n$ |
| $m \sim 4, n \sim 2$ | $m \sim 4, n \sim 2$ |

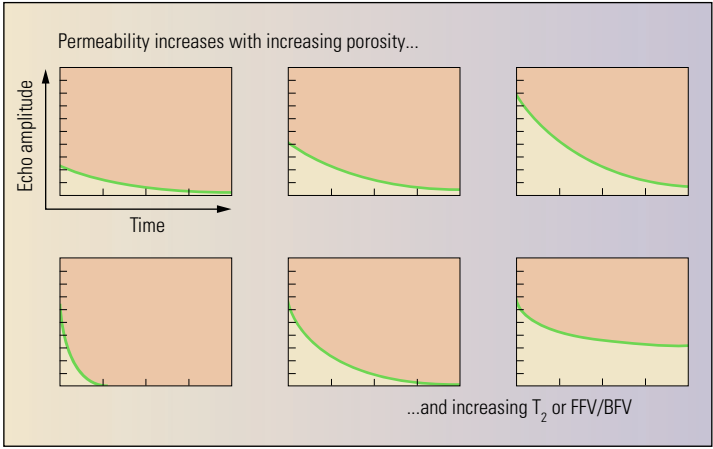
^ NMR permeability transforms. The Timur-Coates equation contains total porosity, ϕ , and the ratio of the free-fluid volume (FFV) to the bound-fluid volume (BFV). The Schlumberger-Doll Research (SDR) equation also contains total porosity, but uses a logarithmic mean T_2 (T_{2LM}) in place of the FFV-to-BFV ratio. The exponents are typically 4 and 2, but can vary with local conditions.

measurements, are the Timur-Coates equation and the Schlumberger-Doll Research (SDR) equation (above). The Timur-Coates equation estimates permeability using total porosity and the ratio of the free-fluid volume (FFV) to the bound-fluid volume (BFV). The SDR transform is based on the logarithmic mean of T_2 and total porosity.

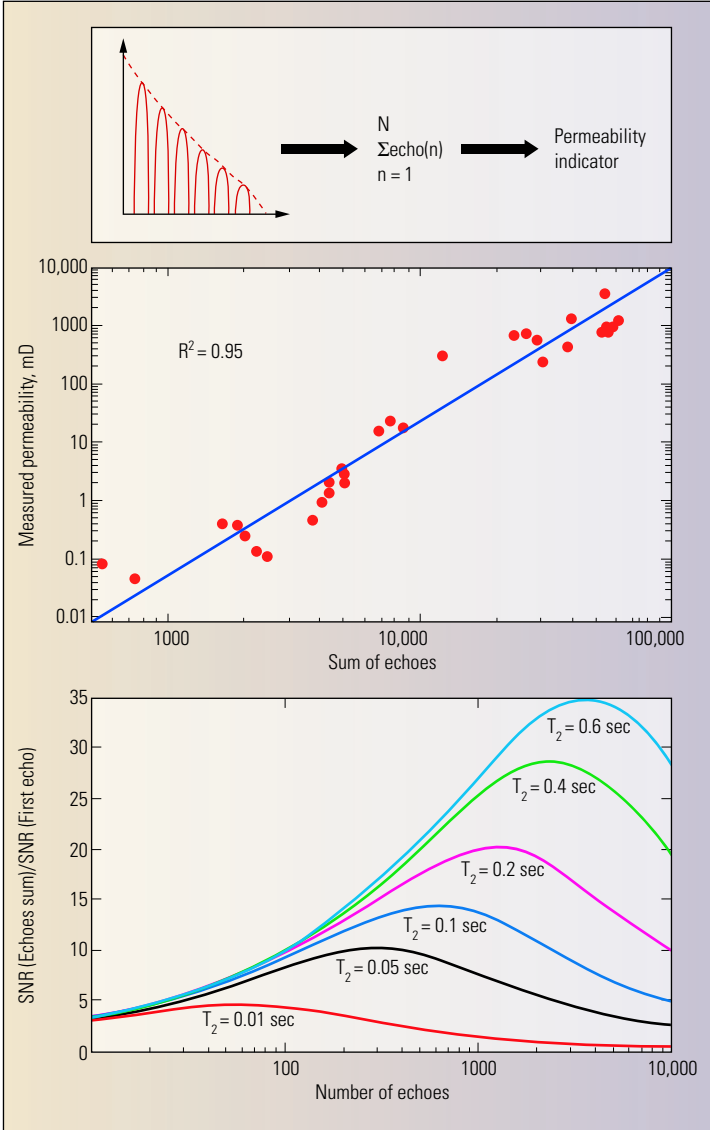
Although the high-resolution porosity processing discussed earlier can be used to derive high-resolution SDR and Timur-Coates permeability, there is an alternative approach that can yield better results in high-noise environments. It has been observed that the sum of all spin-echo amplitudes is proportional to the product of porosity and the average T_2 . This, in turn, correlates well with permeability (above right).⁷ In addition, the sum of echoes has a high signal-to-noise ratio, so it can be interpreted without stacking. This leads to a measurement with higher vertical resolution.

The new high-resolution NMR permeability indicator is derived from the sum of echo amplitudes and is directly proportional to the area under the spin-echo decay envelope (right). The vertical resolution achievable with this novel technique is equal to the tool antenna aperture plus the distance traveled during one CPMG

> NMR high-resolution permeability indicator. The new indicator is simply the sum of the echo amplitudes (top) and is directly proportional to the area of the echo-decay envelope. The high-resolution sum-of-echoes permeability indicator is compared with laboratory-measured permeabilities on 30 core samples from four wells from different parts of the world (middle). The linear correlation ($R^2 = 0.95$) is good for over six orders of magnitude, and compares favorably with that provided by the standard NMR-based permeability transforms. The high-resolution curve shown in the graph was calibrated for a sum of 600 echoes. The prefactor and exponent used in the computation are adjusted according to local conditions. The signal-to-noise gain (bottom), and therefore the optimal number of echoes used in the computation, depends on the T_2 signal-decay rate of the formation.



^ Permeability and the NMR T_2 signal. The top row shows a series of hypothetical NMR signals—echo-decay envelopes—for increasing porosity and permeability in which the T_2 decay time remains constant. The bottom row shows a series of signals in which the porosity remains constant, but the T_2 decay time and computed permeability increase from left to right. The area under the echo-decay envelope and the computed permeability increase with porosity and decay time.



sequence plus the polarization time, typically 7 to 9 in. [18 to 23 cm] for the CMR-Plus tool.

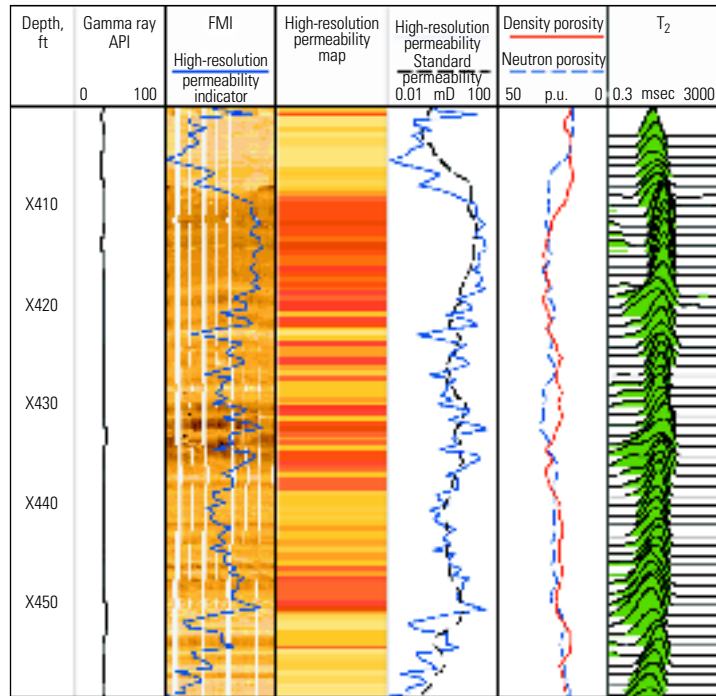
An example from the Ekofisk chalk formation in the North Sea demonstrates the excellent vertical resolution of the new sum of echo-amplitudes permeability indicator (right). While it is widely believed that chalk formations are homogeneous, the FMI images in this well reveal subtle laminations in the chalk. Gamma ray logs, density-neutron logs and the standard five-level stacked SDR transform permeability log with 30-in. [76-cm] resolution offer no indication of these laminations. However, the high-resolution permeability indicator log shows clear permeability variations consistent with the laminations seen in the FMI images.

Improving Well Stimulations

Wells completed in low-to-moderate permeability reservoirs frequently require hydraulic-fracture stimulation to produce at economic rates. Because the fracture treatment often is the main cost driver associated with the completion, operators are looking for ways to ensure cost-effective stimulation designs.

The effectiveness of a stimulation design can be affected dramatically by the permeability of a reservoir. Traditionally, permeability data from whole core, rotary sidewall core and percussion core are used with pressure transient analysis and production history-matching to estimate reserves and design well completions. Documenting production histories requires a time-consuming delay, and is useful only for remedial completions. Acquiring core presents mechanical risks and is often prohibitively expensive. Frequently, laboratory core analysis does not fully represent permeability conditions downhole, and, at best, provides only a small sample that might not be representative of the zone of interest. The preferred method of pressure transient analysis involves a flow period followed by a pressure buildup test, which involves significant personnel and equipment costs. In addition, there are potential workover expenses for running tubing, and the testing process delays post-stimulation production.

Since permeability data usually are sparse, the stimulation engineer may derive a composite permeability. This is typically a bulk-averaged permeability, sometimes from nonrepresentative samples from sweet spots or high-permeability zones. In addition, when continuous detailed permeability data are not available, often the strategy is to design a fracture with only one stage based on the averaged rock strength and permeability of that zone. Frequently, this results in an unrealistic and unsuitable fracture design.



^ Ekofisk chalk formation in the North Sea. The FMI image in Track 2 shows the presence of many thinly laminated chalk beds between X410 and X450 ft. In the FMI image, light yellow indicates resistive low-porosity chalk, and dark brown indicates more conductive, higher porosity chalk. The high-resolution permeability indicator log (blue) is shown in Track 4. The permeability image in Track 3 is derived from the high-resolution permeability indicator log, and it correlates well with the FMI image. In the permeability image, light yellow indicates low-permeability chalk and dark brown indicates higher permeability. The T_2 distributions are shown in Track 6. The gamma ray (black) in Track 1, density (red) and neutron (blue) porosity logs in Track 5, and the standard five-level stacked NMR permeability (dashed black) in Track 4 show little evidence of these laminations.

For example, a nonoptimal stimulation design, based on composite permeability, might produce a fracture of insufficient length and with a large, impractical vertical extent. An optimal design results in creating a narrow and deep conduit into the formation. To improve hydraulic-stimulation models and overcome the traditional limitations inherent in obtaining permeability information, stimulation engineers and operators have been investigating methods of reliably estimating permeability profiles with wireline logs.⁸ Understanding high-resolution permeability distributions across the pay zone optimizes the stimulation treatment because higher permeability streaks can be mapped and correctly included in the fracture design.

NMR-derived permeability can provide accurate, continuous input into a multilayer stimulation design program, such as FracCADE stimulation software. Permeability governs the transport fluid that disappears—called leakoff—into the fresh sandface during a fracture stimulation operation. The leakoff parameter is critical

to fracture design. If the leakoff parameter is set too high, then too much fluid is pumped. This wastes proppant and fluid and results in unnecessary costs. If the leakoff parameter is set too low, then a screenout may occur—resulting in insufficient fracture length and diminished production along with mechanical risks to completions integrity and wasted proppant. Inputting correct permeability data is important. Permeability can easily change by several orders of magnitude within the same sand bed, even while porosity remains constant.

7. Sezginer A, Cao Minh C, Heaton N, Herron M, Freedman R and Van Dort G: "An NMR High-Resolution Permeability Indicator," *Transactions of the SPWLA 40th Annual Logging Symposium*, Oslo, Norway, May 30-June 3, 1999, paper NNN.

8. Fairhurst DL, Marfice JP, Seim MR and Norville MA: "Completion and Fracture Modeling of Low-Permeability Gas Sands in South Texas Enhanced by Magnetic Resonance and Sound Wave Technology," paper SPE 59770, presented at the SPE CERI Gas Technology Symposium, Calgary, Alberta, Canada, April 3-5, 2000.

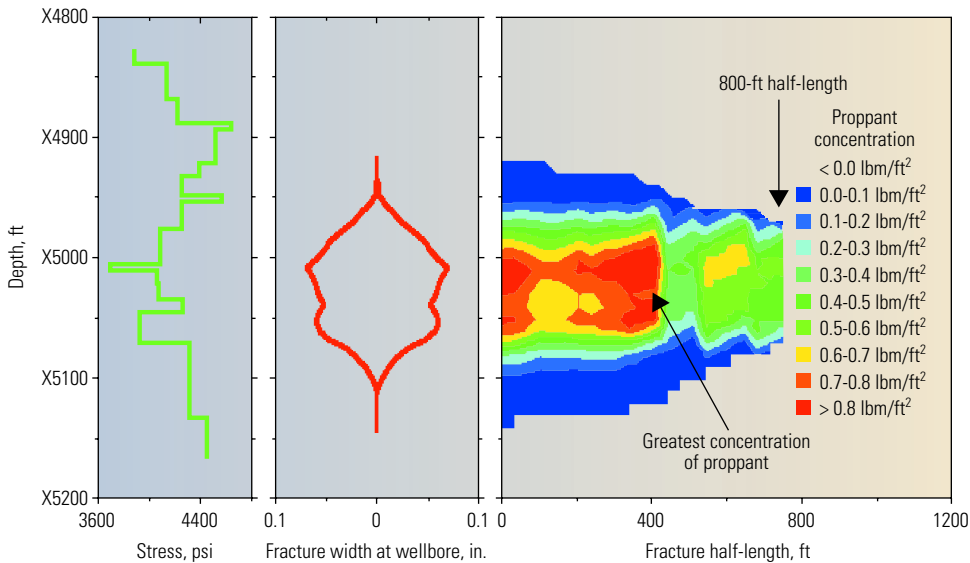
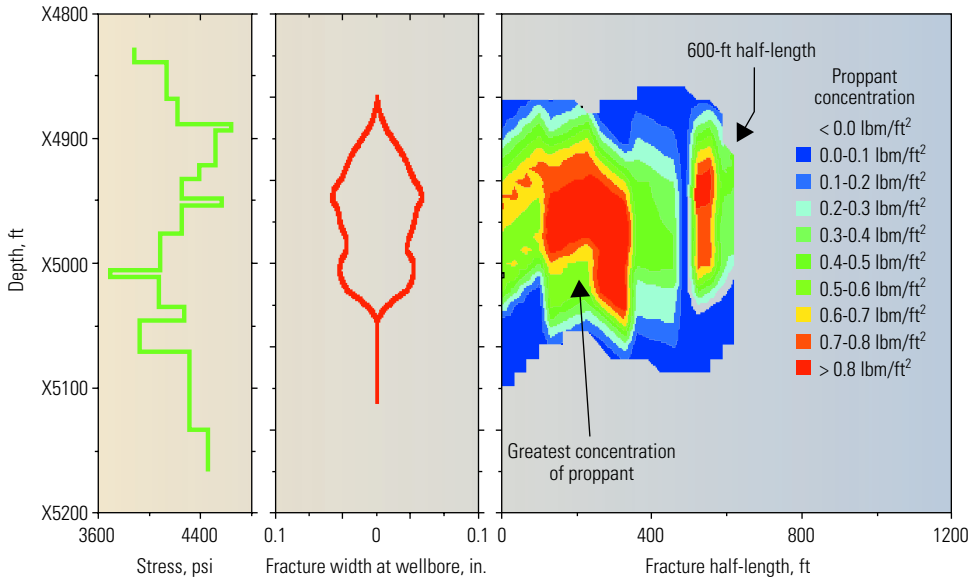
Kerns Oil and Gas, Inc. has been using total CMR porosity and permeability measurements to provide critical input parameters to their stimulation designs for tight gas-sand wells in south Texas, USA. For example, two FracCADE fracture-stimulation designs were prepared for one well (below). Both designs used the same rock strengths and amounts of fluid and proppant. The first design incorporated traditional permeability data from sidewall core estimates and

published data. The resulting high, short fracture design is unsuitable for effective production. The lateral extent of the fracture is 600 ft [183 m] into the reservoir.

A second fracture design, based on the continuous logged NMR permeability data, leads to a longer fracture—penetrating 800 ft [244 m] deep into the formation—with effective proppant placed at least twice as far into the formation as the first design.

If the continuous high-quality NMR permeability data were not available, the stimulation engineer would have been misled by simulation results such as those from the first model. Achieving the desired fracture length would require increasing the pumping schedule—higher pumping rates and increased fluid and proppant volumes. The result is a more expensive and less efficient stimulation job. The possibility of screenout is much higher with the over-designed job. A detailed profile of permeability with depth provided by NMR logs is helping Kerns Oil and Gas continue its remarkable track record of 92% success in achieving or exceeding their production objectives with stimulation treatments (next page, top).

In some cases, the cost of gathering all the data for optimizing fracture geometry prohibits its full implementation, leading to a suboptimal stimulation. Here, continuous NMR permeability data allow the stimulation engineer to consider multistage stimulation designs. For example, the highest permeability zones can be stimulated effectively with a smaller, shorter, lower cost fracture. The payout from immediate production is realized early. Then, after this zone has been under production for some time, the reservoir pressure in the high-permeability zone drops, which results in an increased stress contrast between the gas zone and the shale boundary



▲ Stimulation designs. The FracCADE program was used to compare two fracture stimulation designs in a tight gas-sand formation. The first design (top) used permeability information from core samples and local knowledge. It overestimated the permeability by a factor of 10, resulting in an excessively high and short fracture unsuitable for optimal production. The second design (bottom) was based on detailed continuous NMR permeability logging data. It resulted in a longer fracture, 800 ft [244 m], of limited height more suitable for enhanced gas production. The proppant in the second design was placed twice as deep as that predicted by the first design.

9. Kerchner S, Kaiser B, Donovan M and Villareal R: "Development of a Continuous Permeability Measurement Utilizing Wireline Logging Methods and the Resulting Impact on Completion Design and Post Completion Analysis," paper SPE 63259, presented at the SPE Annual Technical Conference and Exhibition, Dallas, Texas, USA, October 1-4, 2000.

10. The September 21, 2000 gas price was about \$5.28/Mscf.

| Well | Formation | Prestimulation | Estimated from FracCADE prediction | Post-stimulation |
|------|------------|------------------------|------------------------------------|-------------------------|
| 1 | San Miguel | 100 Mcf/D | 400 Mcf/D | 500 Mcf/D |
| 2 | San Miguel | 800 Mcf/D and 25 BOPD | 1200 Mcf/D | 1550 Mcf/D and 200 BOPD |
| 3 | San Miguel | 1000 Mcf/D and 20 BOPD | 1600 Mcf/D | 2000 Mcf/D and 45 BOPD |
| 4 | Olmos | No flow | 200 Mcf/D | 410 Mcf/D |
| 5 | Olmos | No flow | 350 Mcf/D | 370 Mcf/D |
| 6 | Olmos | No flow | 500 Mcf/D | 330 Mcf/D |
| 7 | San Miguel | No flow | 300 Mcf/D | 320 Mcf/D and 18 BOPD |
| 8 | Olmos | No flow | 300 Mcf/D | 340 Mcf/D |

^ Well production results using NMR logging data. Before stimulation, several wells produced no flow. Production estimated using permeabilities derived from NMR logging correlates well with observed post-stimulation production.

layers. This increased stress contrast allows a second fracture stimulation to penetrate deeper into the higher permeability zone without risk of increasing fracture height.

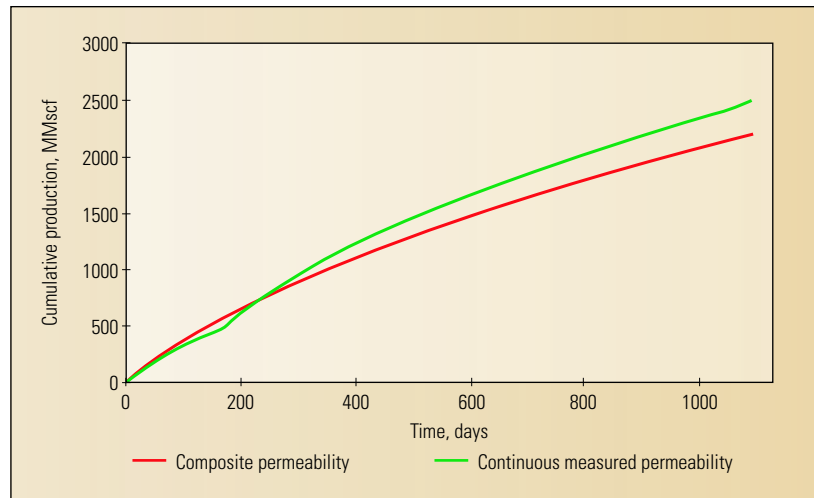
Such an approach was developed by Conoco during a project to understand the economic impact of using continuous NMR permeability data on hydraulic-stimulation projects.⁹ An economic model based on net present value (NPV) was used to test the sensitivity of different variables in the fracture optimization (see "Taking a Calculated Risk," page 20). In one well, a traditional single-stage design required 288,192 gal [1090 m³] of fluid and 935,216 lbm [424,214 kg] of proppant to achieve a 795-ft [242-m] optimum fracture length at a cost of \$320,000. The estimated recovery in three years would total 2.2 Bcf [62 million m³] of gas.

By first targeting the high-permeability zone with a small stimulation treatment and following later with a second treatment in the lower permeability zone, the two hypothetical treatments used a total of 186,383 gal [705 m³] of fluid and 438,079 lbm [198,713 kg] of proppant. The first zone fracture half-length was 388 ft [118 m] and the second was 1281 ft [390 m] at a total cost of \$254,000. The estimated reserves recovery in three years was 2.5 Bcf [70 million m³] of gas

(above). The two-stage stimulation design using continuous NMR permeability data results in a \$66,000 cost-savings and increased production of 292 MMcf of gas, which is worth approximately \$1.5 million at current gas prices.¹⁰

Combining continuous NMR permeability logging data with hydraulic-fracture stimulation designs is one of the objectives of the PowerSTIM initiative, which will be discussed in an upcoming *Oilfield Review* article.

(continued on page 14)



^ Cumulative production of traditional and NMR-based stimulation designs. The cumulative production was computed using ProCADE software based on the height of the net pay, bottomhole static pressure and permeability. The red curve shows the production based on the traditional composite permeability estimates and a single-stage fracture-stimulation design. The green curve is based on the continuous NMR permeability data and a two-stage stimulation design.

Basics of NMR Logging

Modern NMR logging tools use large permanent magnets to create a strong static magnetic polarizing field inside the formation. The hydrogen nuclei of water and hydrocarbons are electrically charged spinning protons that create weak magnetic fields—like tiny bar magnets. When a strong external magnetic field from the logging tool passes through a formation containing fluids, these spinning protons align themselves like compass needles along the magnetic field. This process, called polarization, increases exponentially with a time constant, T_1 , as long as the external magnetic field is applied.¹ A magnetic pulse from the antenna rotates, or tips, the aligned protons into a plane perpendicular, or transverse, to the polarization field. These tipped protons immediately start to wobble or precess around the direction of the strong logging-tool magnetic field, just as a child's spinning top precesses in a gravitational field.

The precession frequency, called the Larmor frequency, is proportional to the strength of the external magnetic field. The precessing protons create oscillating magnetic fields, which generate weak radio signals at this frequency. The total signal amplitude from all the precessing hydrogen nuclei—typically a few microvolts—is a measure of the total hydrogen content, or porosity, of the formation.

The rate at which the proton precession decays is called the transverse relaxation time, T_2 , and is the second key NMR measurement because it reacts to the environment of the fluid—the pore-size distribution. T_2 measures

the rate at which the spinning protons lose their alignment within the transverse plane. It depends on three things: the intrinsic bulk-relaxation rate in the fluid; the surface-relaxation rate, which is an environmental effect; and relaxation from diffusion in a polarization-field gradient, which is a combination of environmental and tool effects.

In addition, the spinning protons will quickly lose their relative phase alignment within the transverse plane because of variations in the static magnetic field.² This process is called the free-induction decay, and the Carr-Purcell-Meiboom-Gill (CPMG) pulse-echo sequence is used to compensate for the rapid free-induction decay caused by reversible transverse dephasing effects.³

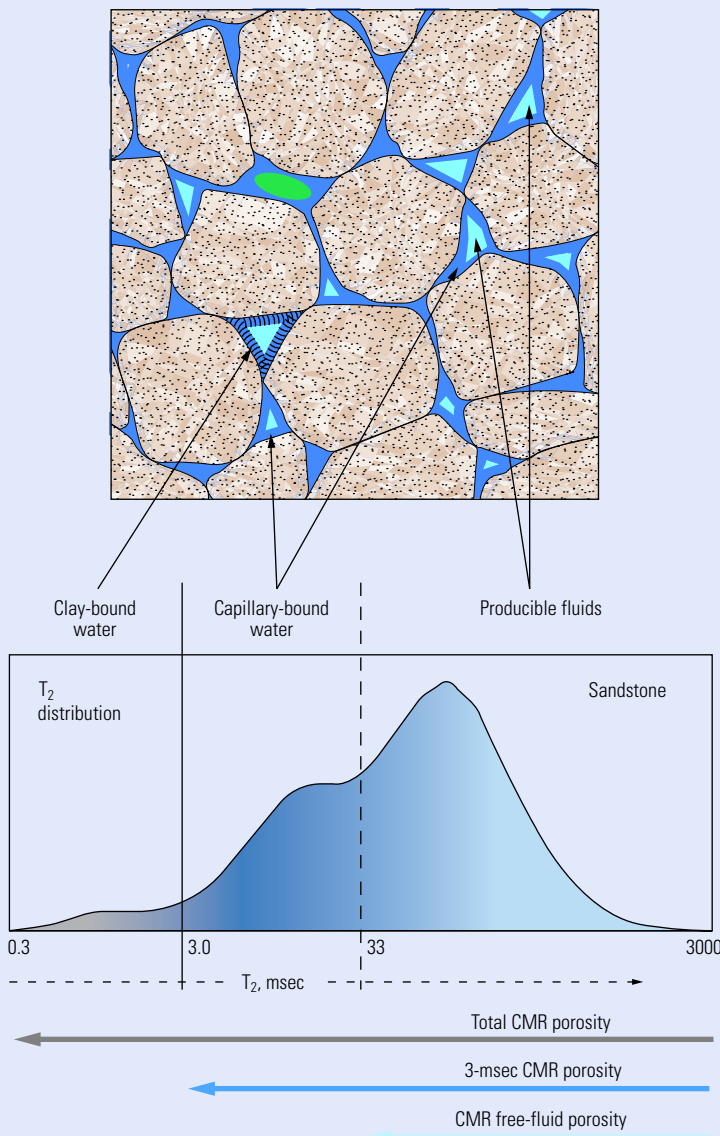
The three components of the transverse-relaxation decay time play a significant role in the use of the T_2 distribution for well-logging applications. For example, the intrinsic bulk-relaxation decay time is caused principally by the magnetic interactions between neighboring spinning protons in the fluid molecules. These are often called spin-spin interactions.

Molecular motion in water and light oil is rapid, so the relaxation is inefficient with correspondingly long decay-time constants. However, as liquids become more viscous, the molecular motions are slower. Then, the magnetic fields, fluctuating due to their relative motion approach the Larmor precession frequency, and the spin-spin magnetic relaxation interactions become much more efficient. Thus, tar and viscous oils can be identified because they relax relatively

efficiently with shorter T_2 -decay times than light oil or water.

Fluids near, or in contact with, grain surfaces relax at a much higher rate than the bulk-fluid relaxation rate. Because of complex atomic-level electromagnetic field interactions at the grain surface, there is a high probability—characterized by the surface-relaxivity parameter—that the spinning proton in the fluid will relax when it encounters a grain surface. For the surface-relaxation process to dominate the decay time, the spinning protons in the fluid must make multiple encounters with the surface—caused by Brownian motion—across small pores in the formation. They repeatedly collide with the surface until a relaxation event occurs.

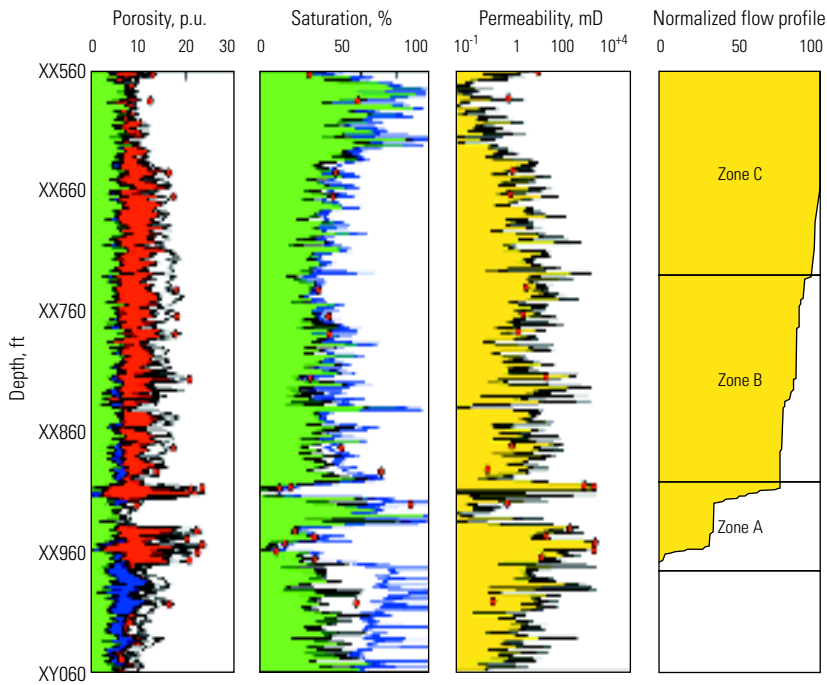
The resulting T_2 distribution leads to a natural measure of the pore-size distribution ([next page](#)). Traditionally, the total porosity seen in formations is subdivided into three major components: free-fluid porosity with long T_2 components, capillary-bound water with T_2 greater than 3 msec and less than the T_2 cutoff for the free-fluid component, and finally, the fast decaying clay-bound water below 3 msec. As NMR tool technology has improved over the last decade with shorter echo spacing, more components of porosity now can be measured, including the fastest clay-bound water signal below 3 msec. Today, for example, the CMR-200 and CMR-Plus tools can measure T_2 down to the 0.3-msec range while logging continuously, and to 0.1 msec during stationary measurements.



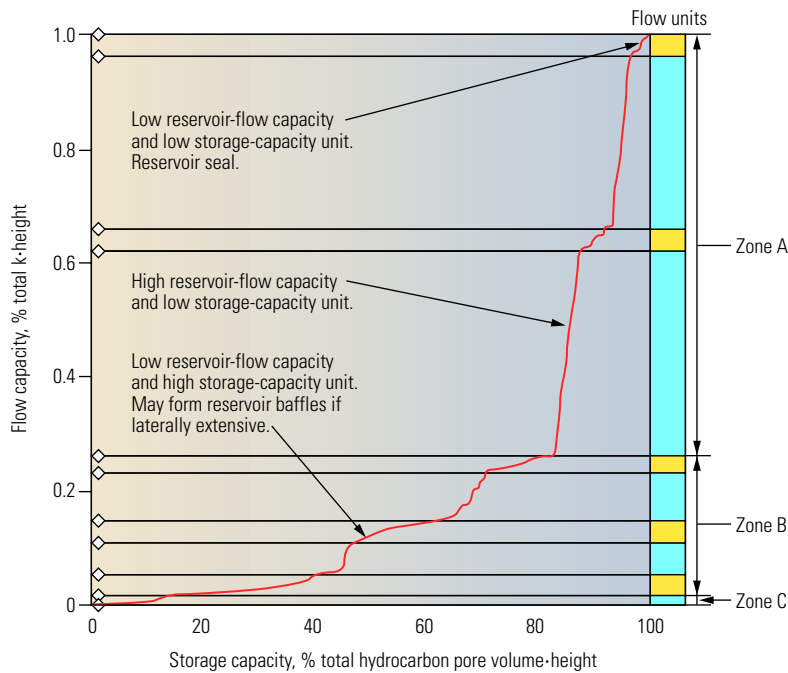
^ Using NMR T_2 distributions (bottom) to identify fluid components (top) in sandstone reservoirs. In water-wet sandstone rock, the T_2 time distribution reflects the pore-size distribution of the formation. Producing fluids include free water (light blue), or pockets of oil (green) in the larger pores. Free water and light oils contribute to the longer T_2 time components. Capillary-bound water (dark blue) is held against sand grains by surface tension and cannot be produced. Clay-bound water (black) is also unproducing. Shorter T_2 time components are from irreducible water that is closely bound to grain surfaces.

Relaxation from diffusion in the polarization-field gradient is a technique frequently used to differentiate oil from gas.⁴ Because the spinning protons move randomly in the fluid, any magnetic-field gradients will lead to incomplete compensation with the CPMG pulse-echo sequence. For example, between spin-flipping pulses, some protons will drift—due to their Brownian motion—from one region to another of different field strength, which changes their precession rate. As a result, they will not receive the correct phase adjustment for their previous polarization environment. This leads to an increase in the observed transverse dephasing relaxation rate. Gas has relatively high mobility compared with oil and water, and therefore, the spinning protons in gas have a much larger diffusion-in-gradient effect. It is important to know that a uniform magnetic-field gradient isn't required to exploit the diffusion-in-gradient effect. All that is required is a well-defined and mapped gradient volume to differentiate gas from oil.⁵

1. The time constant for the polarizing process, T_1 , is traditionally known as the spin-lattice decay time. The name comes from solid state NMR, in which the crystal lattice gives up energy to the spin-aligned system.
2. The observed fast decay, called the free-induction decay, is due to the combined components of irreversible transverse-relaxation decay interactions and the reversible dephasing effect caused by variations in the static magnetic field.
3. The pulse-echo technique used in today's tools is called the CPMG sequence, named after Carr, Purcell, Meiboom and Gill, who refined the pulse-echo scheme. See Carr HY and Purcell EM: "Effects of Diffusion on Free Precession in Nuclear Magnetic Resonance Experiments," *Physical Review* 94, no. 3 (1954): 630-638, and Meiboom S and Gill D: "Modified Spin-Echo Method for Measuring Nuclear Relaxation Times," *The Review of Scientific Instruments* 29, no. 8 (1958): 688-691.
4. Akkurt R, Vinegar HJ, Tutunjian PN and Guillory AJ: "NMR Logging of Natural Gas Reservoirs," *The Log Analyst* 37, no. 6 (November-December 1996): 33-42.
5. Flaum C, Guru U and Bannerjee S: "Saturation Estimation from Magnetic Resonance Measurements in Carbonates," *Transactions of the SPWLA 41st Annual Logging Symposium*, Dallas, Texas, USA, June 4-7, 2000 paper HHH.



▲ CMR-derived permeability in the North Sea. Track 1 contains the CMR-derived porosity subdivided into oil (red), capillary-bound water (green), clay-bound water (white) and producible water (blue). Track 2 contains the saturation analysis based on integrating CMR data with resistivity measurements showing irreducible water saturation (green) and total water saturation (blue curve). The CMR-derived permeability is shown in Track 3. Laboratory-measured permeability (yellow) is shown for the core samples (red circles). Track 4 shows the normalized flow capacity over the three zones in the reservoir.

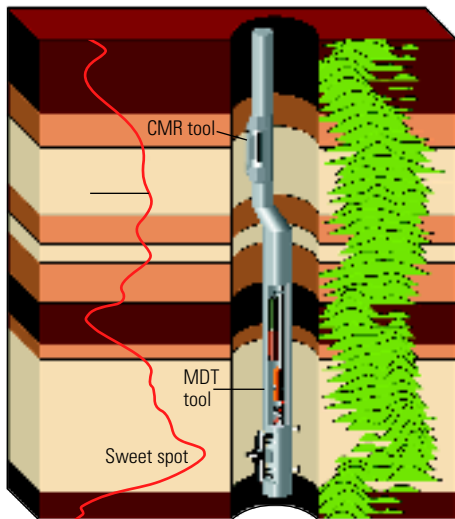


Predicting Reservoir Flow

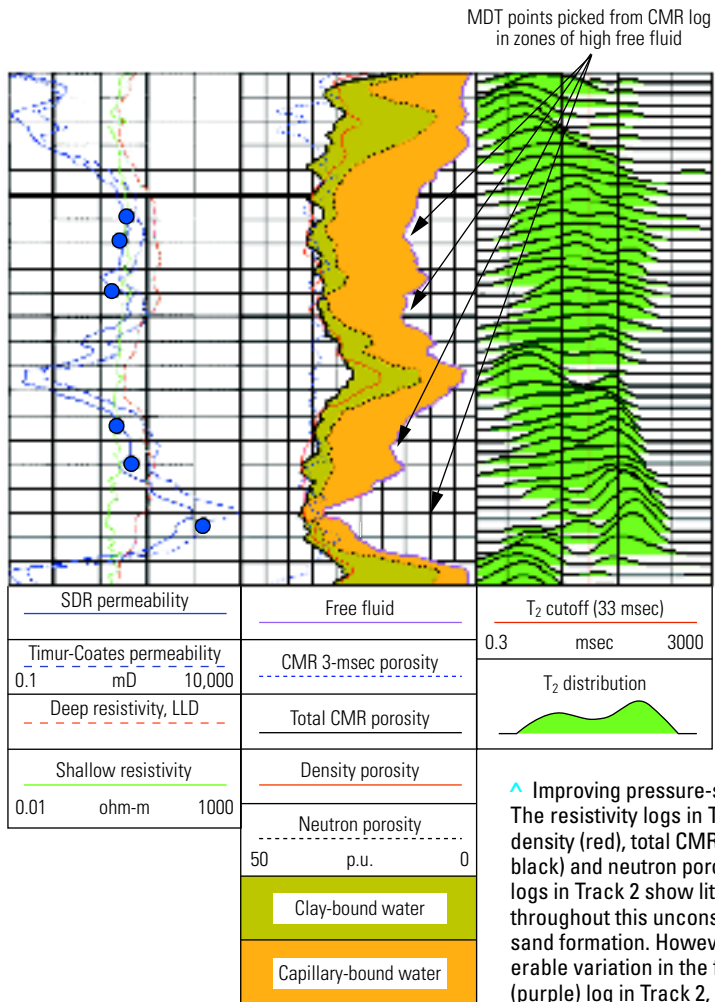
Quantitative petrophysical data are increasingly being applied to numerical simulators for reservoir management.¹¹ For example, CMR measurements were used to help predict flow characteristics in a well in the central North Sea by BG International and Phillips Petroleum. First, laboratory NMR and conventional core analysis were compared to optimize a new NMR-based permeability algorithm. Next, the CMR-derived total porosity and irreducible water were used in the new algorithm to determine permeability continuously across the entire reservoir (left). From this, the flow performance of the reservoir was determined by comparing a plot of the flow capacity, defined by the product of the permeability and thickness, with the storage capacity, defined as the product of the hydrocarbon pore volume and thickness. This graphical tool, called a Lorenz plot, offers a guide to how many flow units are necessary to honor the geologic framework (below left).

The results show that the lowest zone in this well, Zone A, had 17% of the total storage capacity and 74% of the flow capacity. Zone B contained 60% of the storage capacity with 24% of the flow capacity. The upper zone, Zone C, contained 23% of the storage capacity but only 2% of the flow capacity. These results indicate that when the well is put on production, the initial flow rate will decline sharply as Zone A is depleted. The long-term performance of the well will be dominated by production from Zones B and C. Furthermore, a detailed analysis of the plot indicates that a minimum of ten flow units should be employed in the development of the reservoir model. CMR-derived permeability and porosity helped define the flow and storage capacities of each of these ten reservoir units.

◀ Lorenz plot—flow performance based on CMR-derived permeability. The shape of the plot is indicative of the flow performance of the well and reservoir. Segments with steep slopes have a greater percentage of the reservoir flow capacity relative to the storage capacity, and by definition have a higher reservoir production rate. Segments with flat slopes have a higher storage capacity, but little flow capacity, and therefore may form reservoir baffles if laterally extensive. Similarly, segments with neither flow or storage capacities are reservoir seals if laterally extensive. Individual flow units (right column) can be identified from the location of inflection points. These plots can help define the minimum number of flow units to use in the development of reservoir models.



^ Combining NMR logging with MDT downhole formation testing. Choosing formation testing and sample points on the basis of NMR log data provides a reduced margin of error whenever the two tools are run together. Running the two tools together improves efficiency and reduces the risk of deteriorating borehole conditions. The CMR high-resolution permeability indicator helps identify permeability streaks for sweet-spot positioning of the MDT tool.



^ Improving pressure-sampling efficiency. The resistivity logs in Track 1 and the density (red), total CMR porosity (solid black) and neutron porosity (dashed black) logs in Track 2 show little variation throughout this unconsolidated shaly-sand formation. However, there is considerable variation in the free-fluid volume (purple) log in Track 2, making it easy to identify zones of high permeability. In Track 1 the NMR permeability estimates from the Timur-Coates transform (dashed blue) and the SDR transform (solid blue) agree well with fluid mobility determined by the MDT drawdown measurements (solid blue circles). Track 3 shows the CMR T₂ distributions. The MDT samples were chosen at points in the formation that had the best NMR log permeability estimates.

NMR and Wireline Formation Testers

Wireline formation testers are used widely to evaluate formation fluids and producibility.¹² Logging tools such as the MDT Modular Formation Dynamics Tester tool provide downhole estimates of permeability in each pay zone based on dynamic-pressure and fluid-drawdown measurements. Fluid samples, permeability and pressure measurements made with these devices often provide the first look at a well's ability to produce. Recent studies using the MDT tool have shown that the OFA Optical Fluid Analyzer module can provide in-situ crude-oil typing for gas/oil ratio, API gravity and coloration estimates. The MDT tool is also capable of determining the pressure, volume and temperature (PVT) behavior of reserves in place.¹³ Knowing these properties forms the foundation for planning efficient field development.

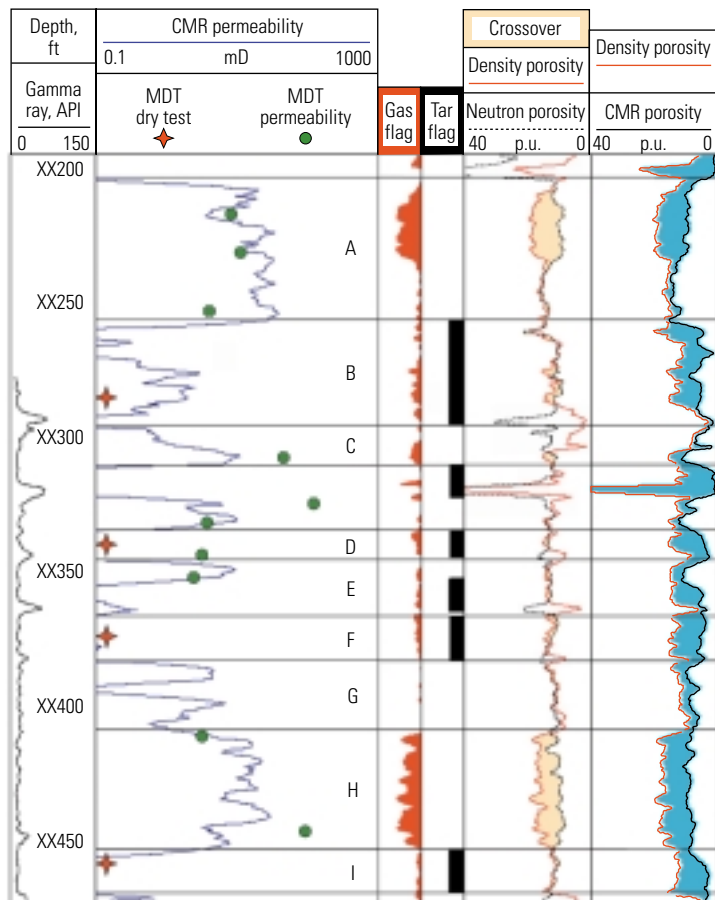
Zone selection is critical in the sampling process. The objective is to obtain a representative sample of the reservoir fluid. Wireline formation tester surveys require stationary measurements and long pumping times to flush mud-filtrate invasion and ensure that PVT-grade formation fluid

samples are obtained. Conventional resistivity-density-porosity logging suites and core data can help identify potential pay zones. However, it is critical to determine correctly which zones will be permeable; otherwise, the tester will not be able to draw any fluid from the formation, or the sampling will take excessive time.

Sampling efficiency can be improved by using NMR permeability measurements to select the most productive zones for sampling (above left). CMR bound- and free-fluid logs also help determine the best points for obtaining MDT pressure measurements and samples. High-resolution CMR data are especially effective in laminated sequences, and high-resolution CMR permeability logging is the recommended practice for determining MDT sampling programs in many locations.

For example, acquiring pressure data in one region offshore China had been problematic because of probe plugging in unconsolidated shaly-sand formations (above right).¹⁴ Although the resistivity and density-neutron porosity logs showed little variation throughout the formation, the CMR free- and bound-fluid logs show substantial variations—making it easy to identify

- Gunter GW, Finneran JM, Hartmann DJ and Miller JD: "Early Determination of Reservoir Flow Units Using an Integrated Petrophysical Method," paper SPE 38679, presented at the SPE Annual Technical Conference and Exhibition, San Antonio, Texas, USA, October 5-8, 1997.
- Crombie A, Halford F, Hashem M, McNeil R, Thomas EC, Melbourne G and Mullins D: "Innovations in Wireline Fluid Sampling," *Oilfield Review* 10, no. 3 (Autumn 1998): 26-41.
- Hashem MN, Thomas EC, McNeil RI and Mullins OC: "Determination of Hydrocarbon Type and Oil Quality in Wells Drilled with Synthetic Oil-Based Muds," paper SPE 39093, presented at the SPE Annual Technical Conference and Exhibition, San Antonio, Texas, USA, October 5-8, 1997.
- Felling MM and Morris CW: "Characterization of In-Situ Fluid Responses Using Optical Fluid Analysis," paper SPE 38649, presented at the SPE Annual Technical Conference and Exhibition, San Antonio, Texas, USA, October 5-8, 1997.
- Castelijns C, Badry R, Decoster E and Hyde C: "Combining NMR and Formation Tester Data for Optimum Hydrocarbon Typing, Permeability and Producibility Estimation," *Transactions of the SPWLA 40th Annual Logging Symposium*, Oslo, Norway, May 30-June 3, 1999, paper GG.



▲ Evaluation of gas, oil and tar zones. The density-derived porosity (red) and neutron porosity (black) logs are shown in Track 3. A tar flag (black) in Track 2 is derived by comparing the density-neutron porosity (Track 3) and the CMR porosity deficit log (Track 4). The gas flag (red) in Track 2 is computed by comparing the volume of gas seen by the CMR tool and that seen by the density-neutron crossover. The CMR log confirms that Zones A, C and H are gas-bearing. The CMR porosity deficit log (blue shading) computed from the difference between density porosity and the CMR porosity is shown in Track 4. Track 1 shows the permeability derived from the total CMR porosity and bound-fluid measurements using the Timur-Coates equation. The ten MDT permeability measurements (green circles) in the high-permeability zones agree well with the CMR-derived permeability log. The four MDT measurements in the tar zones (red stars) were dry (unproductive) tests.

the most permeable intervals. The MDT sample points were selected on the basis of the highest permeability, which are the zones with low bound-fluid volume. All six pressure tests were made successfully, and three fluid samples were recovered in a traditionally difficult sampling environment.

Combining the MDT and CMR tools in one logging pass reduces operating and rig time, resulting in substantial savings, especially in pipe-conveyed, offshore and remote operations. Limiting operating time also reduces the risk of stuck pipe as hole conditions deteriorate.

Fluid characterization—Pressure measurements and fluid-sample analysis combined with specific NMR data signatures—such as long T_2 times in light-hydrocarbon environments or a deficit in the NMR total porosity in tar zones

compared with density-neutron logs—can provide positive identification of formation fluids.

For example, the CMR-MDT combination was run in a well drilled with oil-base mud in the North Monagas area of eastern Venezuela to validate hydrocarbon identification (above). The gas-corrected formation porosity was determined using the DMR Density-Magnetic Resonance Interpretation Method.¹⁵ Interpretation based on density-neutron and CMR data confirmed that Zones A, C and H are gas-bearing. The other zones in this field have no density-neutron crossover and have been interpreted as oil-bearing. However, Zones B, D, E, F and I show large CMR-porosity deficits (shaded blue) in Track 4 compared with density porosity and are interpreted as tar-bearing. Tar has high viscosity and relaxes the NMR signal

quickly. Unfortunately, the resistivity logs cannot distinguish between tar and lighter hydrocarbon zones in this oil-base mud environment.

However, independent confirmation of tar zones was provided by the MDT measurements—all four attempts to sample fluids in these zones with the MDT tool resulted in dry tests. In contrast, all MDT measurements in the gas or light-oil zones produced pressure and mobility readings that agree with the CMR permeability log derived from the total porosity and bound-fluid measurements. CMR-MDT data in combination with triple-combo log data provided a conclusive petrophysical analysis of the complex gas, oil and tar formation.

In four deepwater Gulf of Mexico wells drilled in the same structure, the CMR tool was combined with the MDT tool to confirm locations of fluid contacts in the reservoir. The tools were run in deviated wellbores on drillpipe using a TLC Tough Logging Conditions system, while traditional openhole logs were obtained using logging-while-drilling (LWD) measurements. In one well, the MDT pressure data and the pressure-gradient trends show evidence of a gas-oil contact (GOC) at X270 ft, which is consistent with the porosity deficit of the NMR measurement in the gas zone (next page, bottom). Similar results were found in each of the other wells.

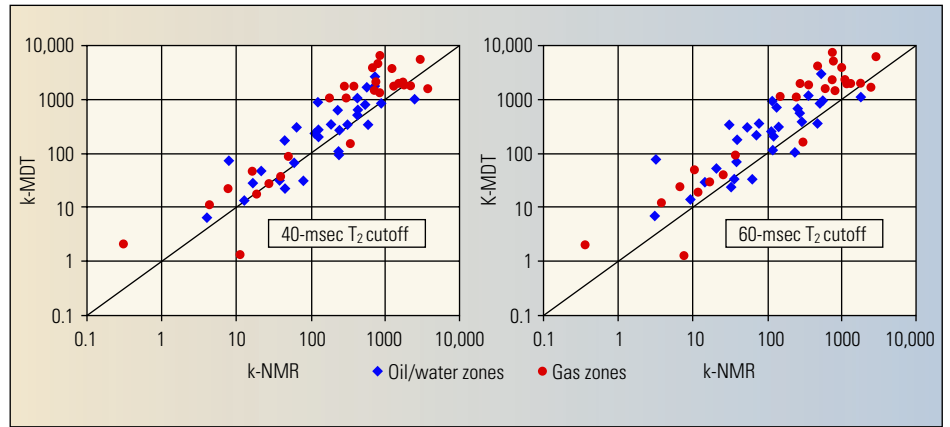
The total CMR porosity overlies the LWD porosity measurement in the water zone below X335 ft, indicating that the protons in the invading mud filtrate—a synthetic oil-base mud system—are fully polarized. In the oil zone from X270 to X335 ft, the total CMR porosity reads lower than the density porosity because of incomplete polarization of the light reservoir oil. The T_2 distribution over this zone indicates an oil signal with an average T_2 in the range of 2 to 3 seconds and a downhole oil viscosity of around 0.3 centipoise, which agrees well with laboratory measurements of MDT samples obtained from this zone.¹⁶ The density-CMR porosity overlay shows increased separation above the GOC at X270 ft. The use of NMR data confirms the interpretation of the MDT pressure data, provides fluid identification and helps establish the location of each fluid contact.

The MDT permeability derived from draw-down-pressure measurements was used in the four-well study to determine the correct T_2 cutoff for differentiating bound fluid from free fluid. The T_2 distributions in each of the wells display a bimodal shape that is commonly seen in wells drilled with oil-base mud systems. Providing the formation is water-wet, the higher peak in the T_2 distribution comes from invaded oil-base mud filtrate and reservoir hydrocarbons, which decay

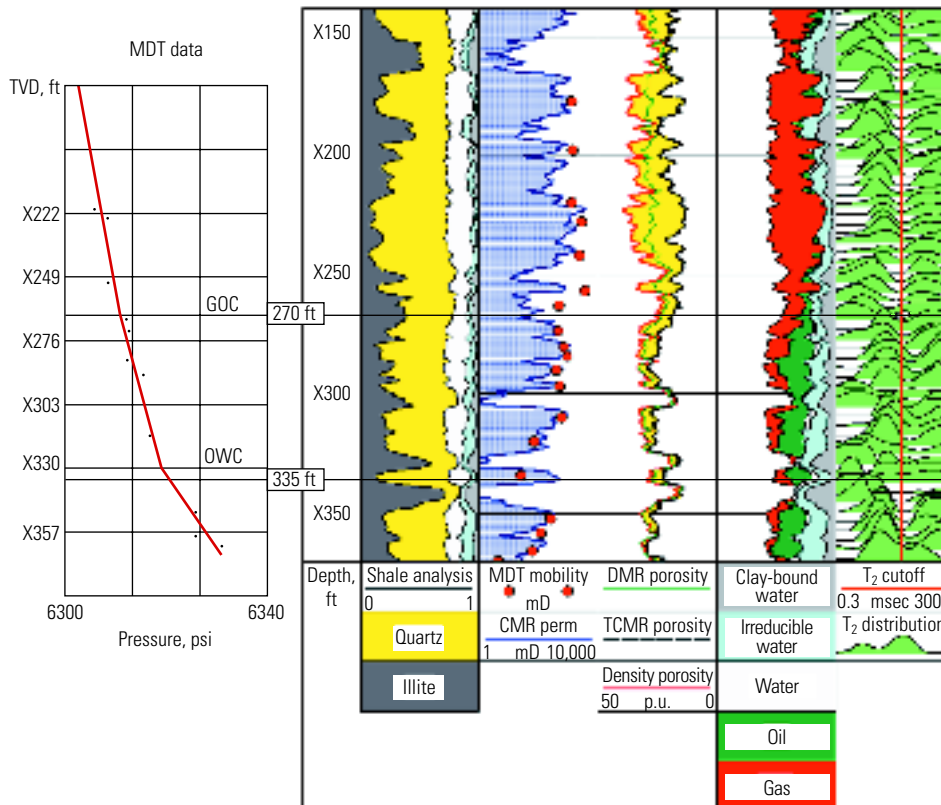
at their bulk-relaxation rates. The lower peak represents the bound fluid. A reasonable estimate for the T_2 cutoff is given by the position of the valley between the two peaks. In these T_2 distributions, the valley appears to be between 60 and 70 msec, whereas typical T_2 cutoff values derived from NMR measurements on core samples from the same formations were only 11 msec.

To establish the correct T_2 cutoff value for this formation, two approaches were tried. First, the T_2 cutoff value was varied to determine the amount of irreducible and free water from the logs in the hydrocarbon zones. The core-derived T_2 value of 11 msec produces a considerable amount of unexpected free water, and the cutoff needs to be increased to 40 msec to remove all the free water in the hydrocarbon zone. Similar discrepancies have been seen in other reservoirs.¹⁷

In the second approach, an optimal cutoff value was determined by varying the T_2 cutoff



^ NMR permeability compared with pressure drawdown permeability. The NMR permeability was derived using the Timur-Coates equation. The effect of varying the T_2 cutoff to discriminate between the free- and bound-fluid components was investigated. The two plots show the effect of varying the cutoff from 40 msec (left) to 60 msec (right). The data in the gas zone show a wider spread, possibly due to the fact that gas can alter the viscosity of the invading fluid, causing error in the MDT permeability derived from drawdown measurements. The optimal correlation was found for the 40-msec T_2 cutoff comparison.



^ Finding fluid contacts. The MDT pressure data plot (left) shows the pressure-gradient changes due to fluid contacts. The gas-oil contact (GOC) is at X270 ft and the oil-water contact (OWC) is at X335 ft. The formation volume analysis is shown in Track 1 (right). The NMR-derived permeability (purple) is compared with MDT drawdown-measured mobility (red circles) in Track 2. In Track 3, the density-derived porosity (red) is compared with the total CMR measured porosity (black). The gas-corrected formation porosity (green) shown in Track 3 was computed using the DMR Density-Magnetic Resonance Interpretation Method. A complete fluid analysis based on the CMR free-fluid, bound-fluid, DMR porosity and other openhole data is shown in Track 4. The CMR-derived T_2 distributions are shown in Track 5.

and comparing the resulting Timur-Coates permeability values with the MDT drawdown permeability measurements (above). Varying the T_2 cutoff changes the NMR-derived permeability profile in each well, as the bound-water volume will vary at different depths.¹⁸ The NMR-derived permeability profile using a 40-msec T_2 cutoff best fits the MDT permeability measurements in this study.

Wellsite-computed NMR permeability can be used to optimize the design of the formation tester pressure measurements and fluid sampling, and better evaluate the production potential in each well.

15. Freedman R, Cao Minh C, Gubelin G, Freeman J, McGinness J, Terry B and Rawlence D: "Combining NMR and Density Logs for Petrophysical Analysis in Gas-Bearing Formations," *Transactions of the SPWLA 39th Annual Logging Symposium*, Keystone, Colorado, USA, May 26-29, 1998, paper II.
16. Morriss CE, Freedman R, Straley C, Johnston M, Vinegar HJ and Tutunjian PN: "Hydrocarbon Saturation and Viscosity Estimation from NMR Logging in the Belridge Diatomite," *Transactions of the SPWLA 35th Annual Logging Symposium*, Tulsa, Oklahoma, USA, June 19-20, 1994, paper C.

- For a discussion of viscosity effects on relaxation time: see Allen et al, reference 1.
17. Allen et al, reference 1.
 18. Effects of varying and unknown fluid viscosity on MDT drawdown mobility measurements were minimized by comparing data only in oil and water zones and avoiding gas zones, where gas dissolved in the invading filtrates could alter fluid viscosity. The effects of differing vertical resolution in comparing the values of CMR-derived permeability with those from the MDT measurements were minimized by eliminating data close to bed boundaries. The leading coefficient in the Timur-Coates equation was adjusted to calibrate the NMR permeability to the drawdown permeability.

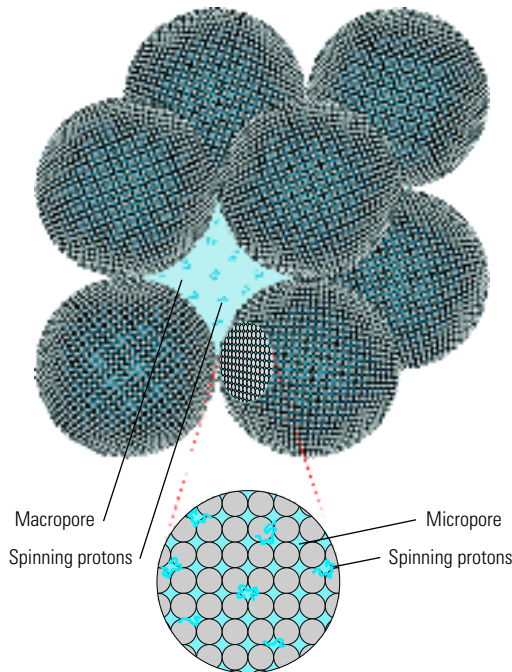
NMR in Carbonates

One of the benefits of NMR-measured porosity is that it is independent of the mineralogy of the formation rock. The echo amplitudes depend only on the hydrogen content of the formation fluids, and are not affected by the rock bulk properties like density or neutron cross sections. This helps to make a petrophysical analysis in complex mineralogy—such as evaluating water saturation in limestone with anhydrite inclusions—much easier.

However, there is some concern within the industry that NMR doesn't work as well as expected in carbonate reservoirs. The problem centers on uncertain mapping between T_2 distributions and pore-size distributions in carbonates. This results in inconsistent T_2 cutoff values needed to distinguish bound and free fluids, and leads to unreliable permeability and water-cut predictions. Some of the suspected causes are diffusion of spinning protons between micro- and macropores, variations in surface relaxivity with temperature and mineralogy, and variable, complex pore systems.

Traditional interpretations of NMR measurements in water-saturated reservoir rocks assume that the T_2 distribution and pore-size distributions are directly related.¹⁹ The diffusion of spinning protons between pores is neglected, and the relaxation in each pore is presumed to be controlled by the grain surface-relaxivity coefficient. This interpretation model results in observed relaxation time that depends on two components—the bulk-fluid-relaxation process, which is slow for fluids with high mobility (water and light oil), and the surface-relaxation process, which depends on the ratio of pore volume to surface area. Water, light oil and gas trapped in large pores decay more slowly, whereas fluid confined to pores with a small pore volume to surface area ratio—such as clay-bound fluid—experiences more rapid decay because of frequent surface encounters. This popular interpretation model successfully explains observed T_2 distributions in sandstone reservoirs containing mixed pore-size distributions.

Carbonate formations also contain multiple pore-size distributions—often consisting of micro- or intragranular porosity and macro- or intergranular porosity, as well as isolated vugs.



< Three-dimensional model based on periodic packing of consolidated microporous grains. A numerical model for carbonate grainstones is based on a simple cubic structure containing large grains of microporous grains, which were made up of smaller, consolidated grains whose centers lie on a sublattice. The NMR physics (*insert*), shows that when pores are coupled by diffusion, spinning protons originally in micropores will escape to the macropores where they survive longer. Spinning protons originally in the macropores penetrate into the micropores where they encounter more surface interactions, decreasing their lifetimes.

Nevertheless, logging data in these formations frequently yield unimodal T_2 distributions that limit the capability of the NMR measurement to predict permeability and movable fluid.

Recent developments in NMR research explain why the conventional approach breaks down in grain-supported carbonates which have dual micro- and macropore systems in close proximity (*above*).²⁰ The breakdown is due to diffusion of spinning protons between the micro- and macropores.²¹ This result was verified using numerical simulations and analytical models to assess the physical processes underlying the NMR measurement on rocks with the same characteristics as those typically found in Middle Eastern carbonate reservoirs (*next page, top*). Diffusion causes the area under the short T_2 peak—the porosity fraction associated with micropores—to decrease; at the same time, the position of the higher T_2 peak shifts towards shorter times. Acting together, these two effects tend to merge the two peaks and produce a unimodal T_2 distribution that bears little resemblance to the bimodal distribution one would expect from a dual-porosity system.

Physically, these effects are caused by diffusion of the fluid's spinning protons between the two pore systems. If the surface relaxivity is small enough, then protons originally in the micropores can diffuse back into the macropores before their nuclear spins relax. The decay of these spins then proceeds much more slowly and contributes to the late-time peak, which explains the apparent transfer of porosity from early-time to late-time peaks.

The role of diffusion in carbonates is further complicated by the observation that the T_2 distributions measured in some carbonate formations have a temperature dependence.²² Previous laboratory work on the effects of temperature was based largely on sandstones and concluded that measured decay does not change with temperature, implying that diffusion does not control relaxation in those formations.²³ In some carbonate reservoirs, comparison between borehole and laboratory NMR measurements shows that, although the total porosity agreement is quite satisfactory, the laboratory lifetimes—measured at room temperature—are significantly shifted to shorter values than those observed in logs.

This result has been repeated in laboratory studies of the temperature dependence of NMR in mud-supported carbonate rocks taken from a number of wells in the Middle East (*next page, bottom*). The diffusion process is dominated by a factor called the fluid-diffusion constant. As temperature increases, the diffusion constant changes and leads to a shift in the observed T_2 distributions to longer times.

19. Allen et al, reference 1.

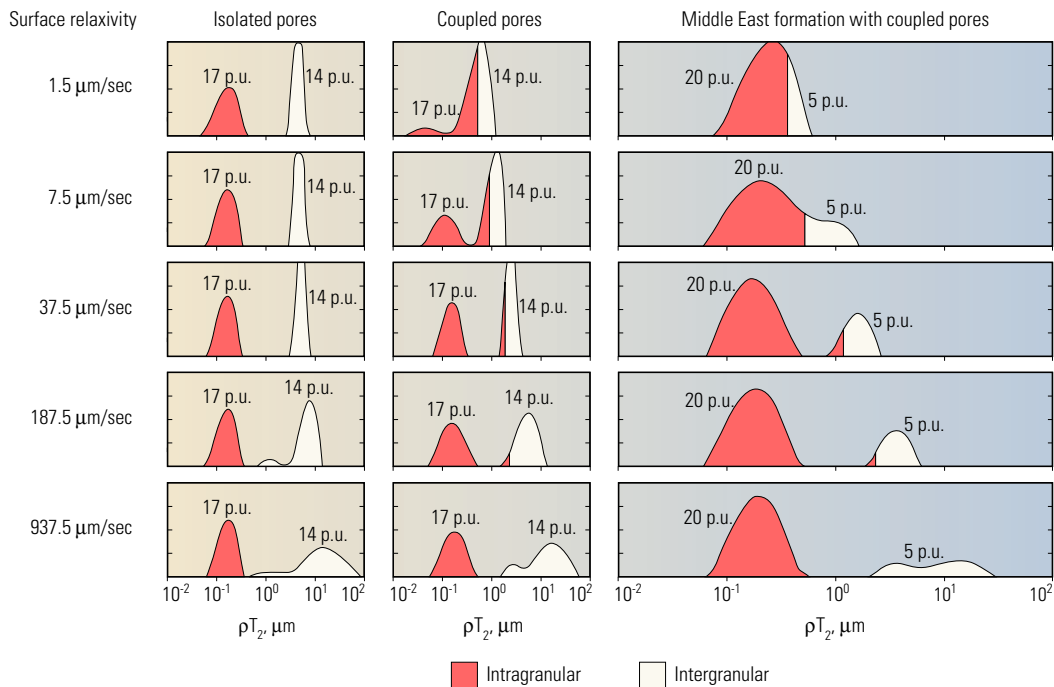
20. Ramakrishnan TS, Schwartz LM, Fordham EJ, Kenyon WE and Wilkinson DJ: "Forward Models for Nuclear Magnetic Resonance in Carbonate Rocks," *The Log Analyst* 40, no. 4 (July-August 1999): 260-270.

21. Typically, the correction for diffusion is due to magnetic-field gradients causing irreversible dephasing. However, even when the field gradient is zero, diffusion can alter the relaxation significantly.

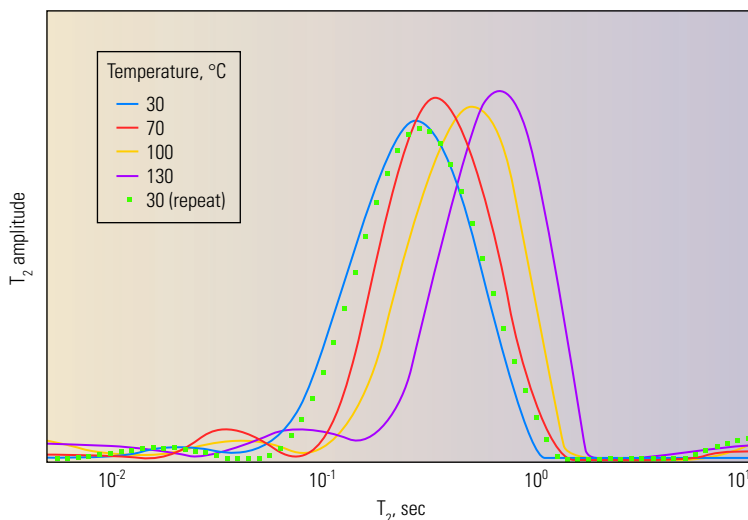
22. Ramakrishnan TS, Fordham EJ, Venkitaraman A, Flaum M and Schwartz LM: "New Interpretation Methodology on Forward Models for Magnetic Resonance in Carbonates," *Transactions of the SPWLA 40th Annual Logging Symposium*, Oslo, Norway, May 30-June 3, 1999, paper MMM.

23. Latour LL, Kleinberg RL and Sezginer A: "Nuclear Magnetic Resonance Properties of Rocks at Elevated Temperatures," *Journal of Colloidal and Interface Science* 50, no. 2 (1992): 535-548.

24. Freedman R, Sezginer A, Flaum M and Matteson A: "A New NMR Method of Fluid Characterization in Reservoir Rocks: Experimental Confirmation and Simulation Results," paper SPE 63214, presented at the SPE Annual Technical Conference and Exhibition, Dallas, Texas, USA, October 1-4, 2000.



Effect of diffusion on inter- and intragranular pore systems. T_2 distributions from simulated grain-supported carbonate formations are shown for a range of surface relaxivities, ρ . In the left column, the T_2 distributions are computed for a formation with 14-p.u. intergranular porosity and 17-p.u. intragranular porosity, that are isolated. The middle column shows the effects of allowing diffusion of protons between the two parts of this dual-porosity system. The right column shows the effect of diffusion on a formation with 5-p.u. intergranular porosity and 20-p.u. intragranular porosity, similar to that seen in many Middle East formations. The two smallest values of the surface relaxivity are representative of those seen in carbonate reservoirs. The x-axis is ρT_2 and has units of length. It reflects typical length scales seen in the rock.



Temperature dependence of carbonate T_2 distribution. Laboratory measurements on a core sample taken from a Middle East carbonate formation show the effect of increasing temperature on the T_2 distribution.

Fortunately, the role of diffusion—with the resultant T_2 distribution distortion—does not affect all carbonates. Depending on the local conditions during deposition, the fabric of younger carbonate formations can vary from grain-supported, in which diffusion effects are significant, to mud-supported carbonates, in which diffusion effects are not expected to be significant. Second, as formations age, the diagenetic overprint usually increases—resulting in increasing crystal

size and decreasing relationship to the original depositional fabric. The decrease in size contrast between pores of close proximity diminishes the effect of hydrogen spin diffusion.

Recent research at Schlumberger-Doll Research in Ridgefield, Connecticut, USA, shows that diffusion is not a factor in either older sucrosic carbonate formations—having a granular texture like sugar—or certain fabric-supported formations. Another finding is that the surface relaxivity in these formations does not vary significantly, and

that NMR distributions exhibit consistent T_2 cut-offs that can be used for estimating permeability. It appears that in these formations, the water molecules remain within either their original micropores or macropores and that interpretations can be performed based on the T_2 distributions, although they differ from the laboratory T_2 distributions due to temperature.

The Next Step

What is next for NMR logging? It is probably a combination of improved technology and greater acceptance by the oil and gas industry. Today, operators are realizing that these tools are no longer high-tech niche players, but instead can give answers that no other tools can, dramatically changing the way wells are completed and reservoirs are developed.

The current generation of NMR tools delivers not only reliable information about formation porosity and permeability, but also supplies rock-characterization information and information about the fluids contained within them. Reliable pore-size distributions are obtained from T_2 distributions measured in clastic sandstone formations.

Despite the progress, many technical challenges remain, particularly in carbonates. What is clear, nonetheless, is that ongoing research and field experience with NMR alone or in combination with other tools will inevitably add more applications, such as better reservoir characterization, for this innovative technology.²⁴ —RH